Submitted: 4th Topical Meeting on Technology of Controlled Nuclear Fusion, King of Prussia, PA, October 14-17, 1980

CONF-801011--82

DESIGN STUDIES OF AN ALUMINUM FIRST WALL FOR INTOR*†

J.R. Powell, J.A. Fillo, W-S. Yu, S-Y. Heieh, Brookhaven National Laboratory, Upton, NY 11973
H. Pearlman, Rockwell International, Canoga Park, CA 91304
R. Kramer, E. Franz, A. Craig, ALCOA, Alcoa, PA 15069
K. Farrell, Oak Ridge National Laboratory, Oak Ridge, TN 37830

Summary

High fluxes of charge exchange neutrals to the first wall are expected for INTOR. These neutrals will have energies in the range of ∿100 to 300 eV, sufficient to cause substantial erosion of the first wall by sputtering. Making the first wall thick enough to survive the integrated neutron wall load of 6.6 MW y/m^2 will result in excessive thermal stresses caused by the cyclical nature of the INTOR reactor operation (nominally 100 sec for the plasma burn, followed by 35 sec dwell) can then occur. Failure of the first wall by fatigue or crack-growth processes, even small local failures, would leak enough coolant into the plasma chamber that the reactor could not operate.

Plasma disruptions also effect the integrity of the INTOR first wall. In existing Tokamak experiments, the plasma sometimes becomes unstable and rapidly dumps its stored energy (thermal and magnetic) onto the plasma chamber. Localized plasma dumps, on a short time scale (typically a few milliseconds), generate very high surface heat fluxes. These heat fluxes are in the range of 10 to 50 kW/cm^2 and can cause serious erosion of the first wall and may cause failure.

Besides the high erosion rates (including evaporation) expected for INTOR, there may also be high heat fluxes to the first wall, e.g., ∿9 (Case I) to 24 (Case II) W/cm^2, from two sources---radiation and charge exchange neutrals. There will also be internal heat generation by neutron and gamma deposition.

An aluminum first wall design is analyzed, which substantially reduces concerns about survivability of the first wall during INTOR's operating life.

Basis for use of Aluminum in INTOR

During the life of INTOR several cm of the first wall may erode from the charge exchange neutral flux and surface evaporation due to plasma disruptions. For a thick bare wall surface, the material should have high-thermal conductivity to minimize surface temperature, temperature gradients, and thermal stresses. The thermal conductivity of aluminum is ∿ 20 times stainless steel, so that aluminum first walls can be much thicker than stainless steel first walls.

The low Z feature of aluminum is also attractive since sputtered impurities will deposit in the plasma and affect plasma performance. Stainless steel sputtering rates, though somewhat smaller than aluminum, are not enough smaller to compensate for much greater impurity effect on plasmas.

Aluminum is easily fabricated into any form including tubes, intricate architectural assemblies, and a wide variety of structural shapes. This is important since the first wall will be contoured to cover the surface of the INTOR plasma chamber.

While it was not a design objective for material selection, aluminum is a very low activation material. Erosion of large amounts of material from the first wall will cause substantial transport of activated materials up beam and vacuum lines leading to the INTOR plasma chamber. Minimizing the activation level of this material appears desirable. An all aluminum first wall blanket system would have great benefits for INTOR. Maintenance and repair operation could be carried out with direct access, rather than remotely as with stainless steel.

Outgassing rates for aluminum and stainless steel are comparable. The maximum aluminum temperature is lower than stainless steel but this should not be restrictive for INTOR applications. The aluminum alloys have a high electrical conductivity relative to stainless steel. This will be significant during plasma disruptions when eddy currents and electromagnetic forces will be induced in the first wall structure. These forces must be taken into account in the design, but do not appear to be an insurmountable problem.

*Work performed under the auspices of the U.S. Department of Energy, Washington, DC 20545.

Design of the INTOR First Wall

The first wall cover-plate, Figures 1 through 3, show a simple structure covering the blanket modules. While tube-like structures are possible, it is much more difficult to header and accommodate thermal stresses.

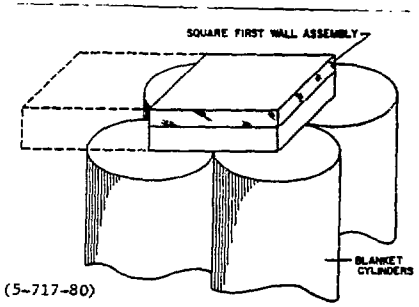

Fig. 1. First wall and blanket arrangement.

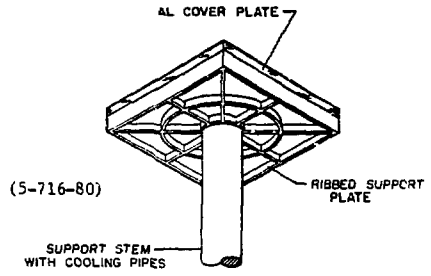

Fig. 2. Aluminum first wall with support plate.

The aluminum cover plate, with coiled or spiral coolant passages, is attached to a ribbed backing or support plate. The central support stem to which the cover and support plates are attached provide the entrance and exit cooling pipes for the first wall cooling. In the square design, a single support stem supports a single first wall plate while in the rectangular design two support stems support a large plate.

To handle higher heat fluxes than those currently projected for INTOR, Figure 4 illustrates another type of first wall design. The first wall is a mosaic of square or hexagonal aluminum plates, suitably curved to cover the surface of the INTOR plasma chamber. Characteristic dimensions of each plate are ~50 to 70 cm

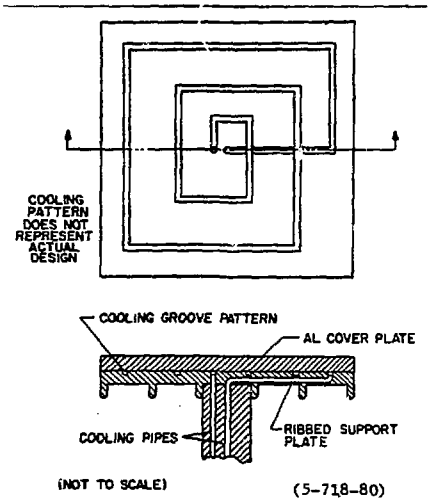

Fig. 3. Schematic of cooling arrangement for segmented aluminum first wall.

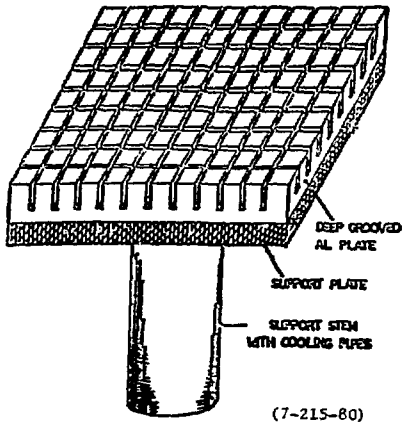

Fig. 4. Segmented aluminum first wall with support plate.

on a side and ~4 cm thick. The front surface of each plate (facing the plasma) is cut to a depth of 2.5 cm by a network of narrow crisscrossing grooves spaced ~2 cm apart. The cuts will reduce thermal stresses in the aluminum plate to low levels.

For the INTOR first wall, commercial aluminum-based magnesium and magnesium-silicon alloys were selected. Besides the advantages inherent in any commercial aluminum alloy for this application (availability, fabricability, good thermal conductivity and heat capacity), these alloys offer several desirable characteristics. The aluminum-magnesium alloys, for example, exhibit the following: 1. Excellent resistance to corrosion, 2. good forming characteristics, 3. moderate strength, excellent welding ability, and 5. strain hardening ability.

In addition to all of these characteristics, the aluminum-magnesium-silicon alloys develop additional strength with heat treatment and, therefore, may be fabricated as a forged or extruded product. Further, the aluminum-magnesium-silicon alloys may be produced commercially, with minimum effect on mechanical properties, with extremely low iron (or other heavy metal) contents as low activation materials.

Specifically, the aluminum-magnesium alloy, 5083-0, and the aluminum-magnesium-silicon alloy, 6061-T6, are recommended as INTOR first wall material candidates. Selection of these alloys and tempers was based upon several factors. With 5083-0 and 6061-T6, complete data on mechanical properties including strength, fatigue, and creep properties are available for the temperature range in which INTOR is expected to operate. Fracture mechanics are well understood and commerical methods for fabricating the particular shapes required for any of the proposed INTOR first wall designs are available. Radiation damage from nuclear fission reactor experience for these or similar alloys have been published. Data based on commercial experience for hydrogen outgassing characteristics are accessible.

The excellent resistance to corrosion of the 5000-series and 6000-series alloys is one of their most important characteristics. These alloys are resistant to industrial and marine atmospheres, fresh water, high-purity water, and many different chemicals. Welds of the alloys are normally as corrosion resistant as the parent alloys. Under certain conditions of elevated temperature service, the 5000-series alloys contain more than ~3% magnesium such as alloy 5083 which may be susceptible to intergranular, exfoliation or stress corrosion. Elevated temperatures are not harmful in the absence of an electrolyte environment, and have less effect when strain hardening is minimal. Use of the annealed (-0) temper or stress relief annealing after fabrication is recommended for this service. The 6000-series alloys are virtually immune to the problems of stress corrosion and exfoliation corrosion.

Exposure tests of 3003 alloy in distilled water show that good corrosion resistance is exhibited at temperatures up to 250°C. Deionized water is handled in much the same way as distilled water. It was found that after an initial conditioning period, aluminum pickup in the system dropped to a negligible value. In a nuclear power plant, tanks fabricated from 5052 alloy have provided several years of continuous service in storage of high-purity water.

Aluminum is widely used in high vacuum systems because of its low outgassing rate and absence of the need for high temperature takeout. A number of large space simulation chambers have been constructed of aluminum alloys. A notable example is the large chamber at the NASA-Lewis Research Center.

ALCOA Research Laboratories compared the outgassing rates of Type 304 stainless steel and 5083 aluminum alloy. Figure 5 compares the rates after bakeout at various temperatures.[1] The outgassing rate 7×10^{-12} Torr-l/sec-cm^2 for 5083 alloy after 127°C bakeout compares with 1×10^{-10} Torr-l/sec-cm^2 for stainless steel after 200°C bakeout. Preliminary tests on the aluminum alloys 2219, 3003, 6061, and 6063 indicate that outgassing rates are comparable to the rates for 5083.

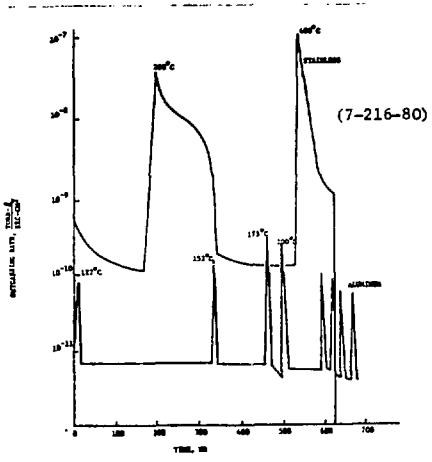

Fig. 5. Outgassing rates, stainless steel and aluminum.

Analysis of the residual gases by means of a mass spectrometer indicate quantities of hydrogen, water, and carbon monoxide and/or nitrogen. Very little carbon dioxide was observed. After 200°C bakeout some hydrogen, a very small amount of water, and a quantity of carbon monixide and/or nitrogen could be observed. From these results, it appears that aluminum can be employed in ultra-high vacuum apparatus. Pumping equipment for aluminum systems need not be any larger than for

comparable stainless steel systems since outgassing rates are comparable.

Response of Aluminum First Wall Under Normal Operation

Thermal Response

The first wall is made up of square or hexagonal aluminum plates. Figure 1 is suitably curved to cover the surface of the INTOR plasma chamber. Characteristic dimensions of each plate are ∿50 to 70 cm on a side and ∿3 cm thick to the coolant passages. Water coolant passages in the base of the aluminum plate maintain the temperature within allowable limits.

For the conditions shown in Table 1, velocities, Reynolds numbers, heat transfer coefficient, pressure drop, and maximum surface temperature are shown as a function of surface heat flux. Two types of operation for INTOR have been examined, as developed by the INTOR design study.

As a consequence of potential corrosion problems, the maximum coolant velocity should not exceed ∿3 m/sec. As Table 1 indicates, this condition can be met with reasonable heat removal characteristics, i.e., duct size, maximum temperature, etc. The Reynolds numbers indicate that the flow will be turbulent. In all cases, pressure drops for a 100-cm flow length are well under an atmosphere. The maximum surface temperatures, Table 1, emphasize the effect of: (a) changing the radial passage dimension, and (b) the change in heat transfer coefficient as the flow passage area is decreased. Decreasing the flow passage area increases the velocity and heat transfer coefficient but decreases the maximum surface temperature.

Representative calculations of the temperature distribution in the first wall have been performed using the heat transfer code, HEATING-V. The plasma was assumed to be "on" for 100 sec and "off" for 35 sec.

Figure 6 indicates typical temperature profiles as a function of time for the first wall surface and surface in contact with the coolant passages for a specific "x" location. There is very little variation with x so that the problem is essentially one-dimensional. After a single period, the temperature reaches a steady, periodic behavior, i.e., repeats itself. Maximum surface temperature climbs from the bulk coolant temperature to a steady-state value within 40 sec and maintains this value until the end of the plasma burn. It then decreases exponentially to the bulk coolant temperature until the end of the plasma dwell.

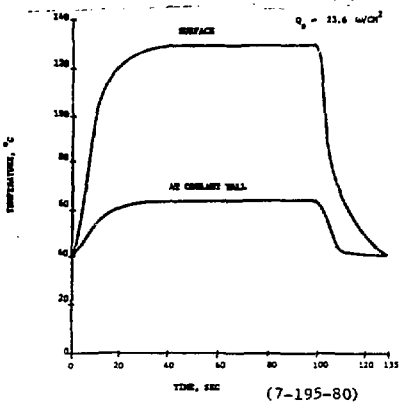

(7-195-80)

Fig. 6. First wall temperature distributions.

Table 1. Comparative Study of Thermal Hydraulic Parameters.

Common Design Parameters				
50 cm x 50 cm plate Coolant flow length = 100 cm Thickness of plate = 4 cm		Volumetric n + γ heating = 8 w/cc $T_{coolant}$ (inlet) = 40°C, ΔT = 10°C Prandtl number = 4.3		
Surface Heat Flux				
	INTOR Case I 9.2 w/cm²	INTOR Case II 23.6 w/cm²		
u, m/s	2.8	1.9	3.9	5.5
R_e	2.12×10^4	1.34×10^4	3.0×10^4	3.4×10^4
h, w/cm²°C	1.37	0.96w/cm²°C	1.80	2.35
ΔP, psi	2.81	1	5.2	9.1
T_{max}, °C	104	150	133	125
Coolant flow passage	1/2cm x 1/2cm	1/2cm x 1cm	1/2cm x 1/2cm	1/2cm x 3/8cm

Stress Response

Thermal stress analyses for four cases were made: (1) high flux (Case II) and thick wall (3 cm), (2) high flux and thin wall (2.5 cm), (3) low flux (Case I) and thick wall, and (4) low flux and thin wall. As expected, the high flux and thick wall lead to the highest temperature in the aluminum which is at the heated surface of the wall. The steepest gradient is at the hot-side surface of the water channel where it is expected that the stresses also will be high. The temperature profile across most of the wall is convex upward caused by the internal heat generation. The data supplied by the thermal analysis were used in the subsequent stress analysis. A peak temperature of 175.9°C occurs at a heat flux of 23.6 W/cm^2 and a distance of 3.0 cm between coolant channel edges and the inner wall.

The stress studies were performed using the "ANSYS" program on a CDC Cyber 176 computer.[1] Figure 7 is a plot of the worst case stresses across the wall which occurs when the heat flux is 23.6 W/cm^2 and the wall thickness (inside surface to water channel) is 3.0 cm. Line A intercepts the water channel while line B passes only through aluminum. Line A stresses are compressive at the inner and outer surface but become tensile at the water channel where the stresses reach a maximum of about +6000 psi. Line B has a similar pattern except that the peak stresses in the channel region are only about +3000 psi. The difference is due to the concentration of stress at the channel corners. While circular channels were not analyzed, it is anticipated that peak stresses occur where the aluminum is at its lowest temperature and also that the highest surface stresses are in compression and are located where the aluminum is again at a low temperature.

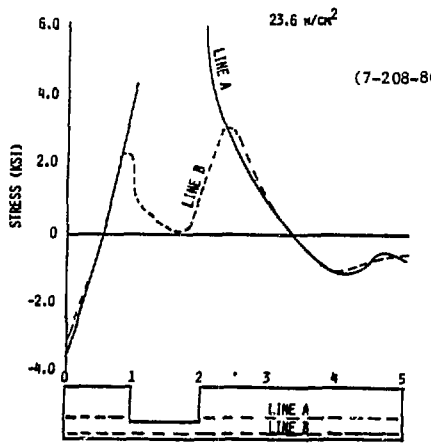

Fig. 7. Stress in aluminum first wall.

The stress levels calculated for all four cases are substantially below the stress limit for 5083-0 alloy at 6x10^5 cycles and the maximum surface temperature, 176°C. The calculated peak stress at this worst case temperature is 740 psi, which is a factor of 25 times below the stress for fatigue failure at 6x10^5 cycles. At interior points in the first wall, temperatures are lower while stresses are higher. The allowable fatigue limit increases somewhat as temperature decreases. At the maximum stress point of 3000 psi (assuming rounded corners in the coolant channels reduce local stress riser effects), maximum allowable stress is 21 ksi, or a factor of 7 above the actual stress. Thus, even for the worst case, stress is far below fatigue limits, however, the possibility of adverse effects of radiation on the alloy properties must be considered. The calculated stress levels appear quite tolerable, but they could be reduced by using cooling channels of circular cross section. The temperature levels, while acceptable for aluminum, could be lowered by the simple expedient of using colder water. This would also reduce adverse effects of radiation.

Erosion Rate Due to Change Exchange Neutrals

As recently pointed out by the Russians, a serious erosion problem exists due to the flux of neutral atoms from the plasma edge of Tokamaks. The resultant sputtering of the wall can seriously limit wall life.

Erosion rate (cm/y) can be estimated from the following equation:

Availability x Duty Cycle x Particle Flux x Sputtering Efficiency (1)

Based on the two projected operating modes of INTOR—Case I involves an efficient divertor, Case II a relatively inefficient divertor--overall average sputtering rates in cm per year have been calculated for INTOR and are summarized in Table 2. Case III refers to peaking of the charge exchange neutral flux near the throat of the divertor and its consequent effect on the local sputtering rate. Calculation of sputtering is reported for a 50/50 deuterium-tritium mixture.

As shown in Table 2, aluminum sputters at about twice the rate of steel; however, the much higher thermal conductivity of aluminum allows aluminum structures to have a much thicker wall and lower thermal stress. Consequently, the aluminum first wall should have a considerably longer life expectancy than a stainless steel wall, based on sputtering resulting from charge exchange neutrals.

The design life of INTOR is twelve years, with an integrated wall load of 6.6 MW-year/m^2; availability is taken as 25% and duty cycle as 70%. Under these conditions, total aluminum erosion is

Table 2. Overall Average Sputtering Rates in cm per year.

Power = Particle Load x Energy

First Wall (380 m^2)	INTOR Case I		INTOR Case II		INTOR Case III		
$\bar{P}$ (MW)	10		10		10		
$\bar{E}$ (eV)	300		300		300		
Flux (part./cm^2-sec)	5.5×10^{16}		8.3×10^{16}		3.2×10^{17}		Local peaking
	Al	SS	Al	SS	Al	SS	
Sputtering rate, cm/y*	0.12	0.05	0.10	0.03	0.73	0.27	
Divertor (20 m^2, assumed)							
$\bar{P}$ (MW)	95				—		
$\bar{E}$ (eV)	1350				—		
Flux (part./cm^2-sec)	2.2×10^{18}		2.2×10^{18}		—		
	Al	SS	Al	SS			
Sputtering rate, cm/y*	3.8	3.2	3.7	2.5			

*50/50 mixture of deuterium and tritium

~1 cm compared with a steel erosion of ~0.5 cm, for the bulk of the first wall. In addition, extra material must be added to reflect loss during plasma disruptions, errors in predicting sputtering rate, and residual strength requirements at end-of-life. These appear to require another ~1 cm material. Thus 2.5 cm thickness of Al would probably be sufficient, which is the thin wall case considered in the thermal/stress analysis. The stresses in this event will thus be substantially less than the thick wall stresses estimated in the analysis above. Although aluminum could function satisfactorily with such a first wall thickness, it appears doubtful that stainless steel could, considering its relatively low thermal conductivity and high thermal stress.

Neither material appears acceptable for use at local peak erosion points, such as those near the divertor entrance (Case III) or on divertor plates themselves. The erosion rates at these points are sufficiently large that periodic replacement is probably necessary.

Response of Aluminum First Wall to Plasma Disruptions

Transient heat reponse during plasma disruptions has also been analyzed for various projected surface heat loads, as listed in Table 3. The corresponding maximum surface temperatures are also listed. Figure 8 indicates first wall surface temperature, as a function of time. The calculations account for melting of the structure, resulting in a phase change or moving boundary problem, but do not include vaporization. Accounting for vaporization would result in reducing the maximum surface temperature, particularly at the peak energy flux of 630J/cm^2. Even so, vaporization losses do not seem to be excessive. For example, for projected surface heat load of 25,000 W/cm^2 applied for 10 msec, the peak surface temperature reached 1350°C, with a melting of the top 0.03 cm during the disruption (Figure 9). The surface fully solidifies within 10 msec after the end of the disruption. Vaporization losses are ~3μg/cm^2 during a disruption. About 10^3 disruptions are expected during the 10^6 pulse lifetime of INTOR (6.6 MW(th) y/m^2) so that the total vaporization loss is insignificant for this condition. Higher heat fluxes, e.g., 31,500 W/cm^2 for 20 msec, results in larger vaporization losses, but these are still not excessive. Stainless steel appears to have much higher vaporization loss rates—due to its much lower thermal conductivity.

Response of Aluminum First Wall to Radiation Damage

Little information is available to predict the response of the aluminum first wall. Studies of fission reactors are dominated by displacement damage (dpa) and transmutation of aluminum to insoluble silicon through (n, γ) reactions. The latter effect will not be important in fusion reactors and first walls because of the hard neutron spectrum and the preferential capture of neutrons by lithium atoms.

Table 3. Projected Surface Heat Loads and Maximum Surface Temperature due to Plasma Disruptions.

Time, msec	Surface Heat Flux, W/cm^2 * 10,500	12,500	25,000	** 31,500
5			950°C	
10			1350°C	
20	850°C	1000°C		

* Average energy flux = 210 J/cm^2, and
** Peak energy flux = 630 J/cm^2.
Time = 20 msec

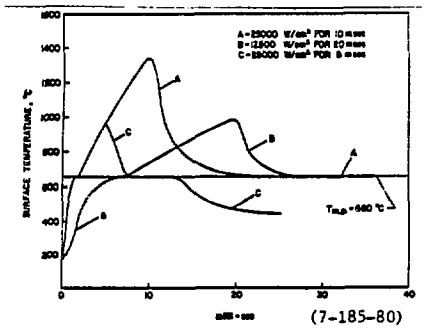

(7-185-80)

Fig. 8. First wall surface temperature as a function of time.

In the fusion reactor environment interstitial gas production, helium and hydrogen, by n,α and n,p reactions will dominate the radiation response. The integrated production of these gases will reach 1000 to 2000 appm (Table 4) over the life of the INTOR first wall for aluminum—somewhat greater than for a stainless steel wall.

Based on fission experience for 6061 and 5052 aluminum to very high dpa (e.g., up to 260 dpa) at 55°C, the displacement damage does not appear to present a serious problem if they are used for the INTOR first wall. The effect of the interstitial gases (primarily helium, since hydrogen is soluble to some extent and much more mobile); however, is potentially of much more concern (as it also is for stainless steel).

Table 4. Nominal INTOR neutron exposure limits for aluminum first wall.

OPERATING MODE	CUMULATIVE (MW-Y/M²)*	DPA	He APPM	H APPM
I + II	1.46	20	461	432
I + II + IIIA	6.64†	93	2098	1965
I + II + IIIB	2.96	41	935	876

*PEAK LOADING (IIIA) = 2.1 MW/M².
†ROUGHLY EQUIVALENT TO 2 x 10^{23}/CM² FLUENCE OF FISSION SPECTRUM NEUTRONS.

Helium has been observed to move to grain boundaries and form bubbles at vacancy sites that seriously degrade ductility and promote cracking, in experiments with dilute ^{6}Li Al alloys and α-implantation. Alloying and precipitates may serve to trap helium and prevent migration, but this has not been studied to any significant degree.

It appears desirable to minimize the potential effect of helium and hydrogen embrittlement by operating the aluminum first wall at relatively low temperatures, i.e., on the order of 150°C.

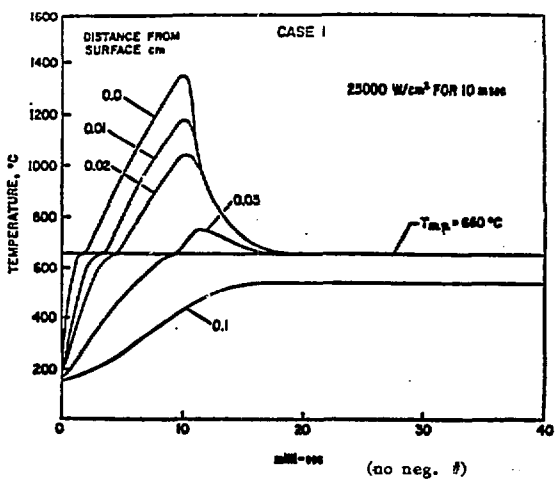

(no neg. #)

Fig. 9. Temperature distribution inside aluminum first wall.

Implications for Future Fusion Reactors

If the erosion rates predicted for INTOR apply to future commercial reactors, it will profoundly affect first wall and blanket design. First, stainless steel would appear to not be a practical material choice for integrated wall loads over ~5 to 10 MW-y/m^2 because of excessive erosion. Second, although aluminum appears to be preferable and could probably function in a practical first wall, it would require operating at a relatively low temperature in the alloy form. [If SAP or fiber reinforced aluminum proved satisfactory, these materials could be operated at high temperature.] This would then require two-temperature-zone blankets with attention paid to maximizing power cycle efficiency. Finally, relatively thick walls would significantly degrade the tritium breeding ratio, requiring careful design to keep breeding at adequate levels.

References

1. Fillo, J.A. Design of an aluminum first wall for the INTOR Reactor, Brookhaven National Laboratory Informal Report, to be published.